Photochemistry and Photobiology, 2013, 89: 432–441

Identification of Ros Produced by Photodynamic Activity of Chlorophyll/ Cyclodextrin Inclusion Complexes

Barbara M. Cellamare[1], Paola Fini[2], Angela Agostiano[1,2], Salvatore Sortino[3] and Pinalysa Cosma*[1,2]

[1]Dipartimento di Chimica, Università degli Studi "Aldo Moro" di Bari, Bari, Italy
[2]CNR-IPCF, sez. Bari, Bari, Italy
[3]Laboratory of Photochemistry, Department of Drug Sciences, University of Catania, Catania, Italy

Received 11 July 2012, accepted 7 September 2012, DOI: 10.1111/j.1751-1097.2012.01238.x

ABSTRACT

Photodynamic therapy (PDT) is a way of treating malignant tumors and hyperproliferative diseases. It is based on the use of photosensitizer, herein the chlorophyll *a* (chl *a*), and a light of an appropriate wavelength. The interaction of the photosensitizer (PS) with the light produces reactive oxygen species (ROS), powerful oxidizing agents, which cause critical damage to the tissue. To solubilize chl *a* in aqueous solution and to obtain it as monomer, we have used cyclodextrins, carriers which are able to interact with the pigment and form the inclusion complex. The aim of this study is to examine which types of ROS are formed by Chl *a*/cyclodextrin complexes in phosphate buffered solution and cell culture medium, using specific molecules, called primary acceptors, which react selectively with the reactive species. In fact the changes of the absorption and the emission spectra of these molecules after the illumination of the PS provide information on the specific ROS formation. The $^1O_2$ formation has been tested using chemical methods based on the use of Uric Acid (UA), 9,10-diphenilanthracene (DPA) and Singlet oxygen sensor green (SOSG) and by direct detection of Singlet Oxygen ($^1O_2$) luminescence decay at 1270 nm. Moreover, 2,7-dichlorofluorescin and ferricytochrome *c* (Cyt Fe^{3+}) have been used to detect the formation of hydrogen peroxide and superoxide radical anion, which reduces Fe^{3+} of the ferricytochrome to Fe^{2+}, respectively.

INTRODUCTION

Photodynamic therapy (PDT) is an efficient alternative treatment both for microbial infections and localized tumors and hyperproliferative diseases. PDT can be used as an alternative or adjuvant to classical therapies, such as radiotherapy, surgery and chemotherapy (1–3). PDT is based on the combined action of a photosensitizer (PS), visible light able to match the absorption spectrum of the PS and endogenous oxygen (4). Following excitation of PS to long-lived excited singlet and/or triplet states, the target tissue is destroyed by reactive oxygen species (ROS), generated in electron-transfer (Type-I mechanism) and energy-transfer (Type-II mechanism) reactions (5). In detail, a Type-I mechanism involves hydrogen-atom abstraction or electron transfer between the excited sensitizer and a substrate, yielding free radicals that can react with oxygen to form ROS such as the superoxide radical anion. While, in a Type-II mechanism, singlet oxygen is generated *via* an energy-transfer process during a collision of the excited sensitizer with triplet oxygen (6).

Photodynamic therapy efficacy depends on photochemical and photophysical properties of PS. Among the different classes of compounds examined as potential photosensitizers in PDT, porphyrins and their analogous are considered the most important because they have photochemical and photophysical properties making them potentially suitable for PDT applications. For example, porphyrins absorption spectra have intense bands in the 600–850 nm wavelength region where the maximum light depth penetration into biological tissues is obtained (7).

The first step of PDT treatment consists in the selective incorporation of the PS into the target tissue. It is normally accepted that tumor selectivity is improved with the increase of the PS lipophilic or amphiphilic character. The drawback of using PSs with such a property is that they have a high tendency to aggregate giving rise to photoinactive forms of the PS, unable to produce ROS. Consequently, a suitable delivery system is required to keep the PS as monomer in solution.

Among the large variety of amphipathic porphyrins, we have carried out a systematic study of the combined use of a natural chlorin, Chlorophyll *a* (Chl *a*), which is the most abundant pigment in green plants, with cyclodextrins.

Chl *a* is insoluble in water because of the presence of a long alcohol chain as an ester moiety (phytilic chain). The magnesium atom in the center of the tetrapyrrolic macrocycle, on the other hand, gives the amphiphilic property to the molecule.

Cyclodextrins are cyclic oligosaccharides characterized by different numbers of α-D-glucopyranose units linked together by *O*-glycoside bonds of types 1–4. Cyclodextrin (CD) toroidal shape, with an inner hydrophobic cavity and an external hydrophilic surface, allows the formation of inclusion complexes with a large number of organic apolar compounds. In fact, CDs are well known as drug delivery systems in pharmacological application. Consequently, the use of CDs as carriers of porphyrins can be useful to shift the equilibrium aggregate-monomer in favor of monomer and then to avoid the aggregation (8–11).

Our previous studies (8–11) have shown that the Chl *a* is effectively solubilized in aqueous environment by means of various

*Corresponding author email: p.cosma@chimica.uniba.it (Pinalysa Cosma)

CDs. In these aqueous systems, Chl *a* results to be much more stable than when it is solubilized using alcohol as cosolvent (12–15). Our studies indicate the formation of inclusion complexes between Chl *a* and CDs characterized by different binding constants and stoichiometry (9,11,16) depending on CD chemical nature taken into exam. Following the structural characterization performed using different techniques (NMR, ITC, UV–Vis absorption and emission), Chl *a*/CD systems have been tested as photosensitizer. The experimental results (16,17) have been shown that almost all Chl *a*/CD systems studied, excited by the absorption of visible light, relax through various photophysical pathways damaging some cellular components leading to cell death (11,16,18). It results that these systems can be considered effective as potential supramolecular systems for PDT applications.

However, for application in oncology, to have phototoxic systems is not enough: the systems have also to be not cytotoxic, feature not required for applications in antimicrobic field. Studies on cytotoxicity have shown that the CD which has the best characteristics for oncological application results to be hydroxypropylated-β-CD (HP-β-CD). This CD is the most effective in Chl *a* solubilization in the cellular medium and also is that which has the lowest cytotoxicity at a 10^{-3} M concentration (17). Higher concentration than 10^{-3} M cannot be used because at increasing of the concentration, all CDs result to be cytotoxic (19,20). At this CD concentration, the highest feasible concentration of Chl *a* as monomer is 10^{-5} M, that is the pigment concentration used in this study.

Although the HP-β-CD is the most appropriate concerning the combined effect of photo- and cytotoxicity, the study was extended to various CDs to have a complete picture on the effect of different CDs on ROS production. In particular, HP-α-CD, HP-β-CD and HP-γ-CD were used for studying the size effect, while the methylated ones for comparing different methylation degree.

Different methods for studying free radical–related processes, as for example the electron paramagnetic resonance (EPR) spin trapping spectroscopy, are difficult to use in cell culture media because of the complexity of the solution media and/or require the use of instrumentations present in specialized laboratories. In fact, the presence, in these systems, of biological molecules could promote the undesirable rearrangement of spin trap adducts and/or their reduction into EPR silent species. This results in a lower sensitivity of the method and in problems with the interpretation of spin trapping data (21). The direct singlet oxygen determination by measuring its luminescence decay at 1270 nm in biological systems is possible, but full of difficulties because of the poor signal–noise ratio in the used ranges of timescales and requires a very sensitive detection systems (22,23). In the laboratories where these sophisticated instruments are not available, the direct near-infrared (NIR)-luminescence detection of produced singlet oxygen *in vitro* or *in vivo* systems often requires the use of deuterium oxide, which increases the lifetime of $^1O_2$ and eliminates absorption of the 1270 nm luminescence by H_2O (24). Hence, the results do not reflect optical and photophysical conditions present *in vitro* or *in vivo* and so should not be interpreted as successful singlet oxygen measurement in a biological environment (24).

To avoid these limits in this study, the identification of different ROS has been carried out by a different approach based on the use of primary acceptors, molecules that selectively react with these species. These reactions change the absorption or emission spectra of these primary acceptors and therefore can be used to demonstrate the production of ROS.

The formation of singlet oxygen in phosphate buffered solution (PBS) solutions and cell culture media (Type-II mechanism) was tested and studied using the reaction of the $^1O_2$ with uric acid (UA) (25–27), Singlet oxygen sensor green® (28) and 9,10-diphenylanthracene (29) (Chart S1). The superoxide radical anion formation (Type-I mechanism) has been detected using its redox reaction with ferricytochrome *c* (Cyt Fe^{3+}), which produces characteristic changes in the cytochrome *c* absorption spectrum (30). Finally, the formation of hydrogen peroxide has been studied using the reaction between the hydrogen peroxide and 2,7-dichlorofluorescin in the presence of peroxidase from horseradish (31) (Chart S1).

MATERIALS AND METHODS

Chemicals. Chlorophyll *a* was extracted and purified from spinach leaves using Omata and Murata method (32). Chl *a* stock solutions were stored in acetone at −80°C. 2-HP-α-CD, 2-HP-β-CD, 2-HP-γ-CD, heptakis-(2,6-di-*O*-methyl)-β-cyclodextrin (DIMEB) and heptakis-(2,3,6-tri-*O*-methyl)-β-cyclodextrin (TRIMEB) used for inclusion complexes have been purchased from Fluka and used without further purification. Cyt Fe^{3+}, 9,10-diphenilanthracene (DPA), D_2O, superoxide dismutase from horseradish, UA and Sodium azide (NaN_3) were purchased from Sigma Company. 2,7-Dichlorofluorescin diacetate (DCFH-DA) and L-Histidine have been purchased from Fluka, singlet oxygen sensor green (SOSG) and 1,4-Diazabicyclo[2.2.2]octane (DABCO) from Molecular Probes and Aldrich, respectively. Cell culture medium without serum was RPMI 1640M from Sigma-Aldrich.

Sample preparation. The inclusion complexes were prepared adding to dry Chl *a,* different CD ethanolic solutions. After ethanol evaporation under N_2 flow, buffer (10^{-2} M, KH_2PO_4/KOH in a range of pH 5.5–9.5) or cell culture medium was added to a final concentration of 10^{-5} M in dye and 10^{-3} M in CD. Subsequently, ROS formation was tested using different primary acceptors: ferricythocrome *c* at a concentration of 0.1 mg mL^{-1}; UA at a concentration of 10^{-4} M; SOSG at a concentration of 1.5 μM; activated 2,7-dichlorofluorescin (DCFH) at final concentration of 40 μM; and finally DPA was used at a concentration of 25 μM. For the test of H_2O_2, the activated DCFH was prepared from DCFH-DA as follows 0.5 mL of DCFH-DA 1 mM (in ethanolic solution) was added to 2 mL of NaOH solution 0.01 N and was stored at room temperature for 30 min in the dark. The DCFH hydrolysate was then neutralized adding 10 mL of sodium phosphate buffer 250 mM at pH 7.2 and was stored in the dark before use. Immediately after the end of irradiation, we added 1 mL of activated DCFH to the analyzing system (33). For the test of H_2O_2, we prepared different types of solutions: Chl *a*/2-HP-β-CD and only 2-HP-β-CD in phosphate buffer solution; Chl *a*/2-HP-β-CD and only 2-HP-β-CD in cell culture medium; Chl *a*/2-HP-β-CD and only 2-HP-β-CD in phosphate buffer solution in which is present a little amount of ethanol; Chl *a*/2-HP-β-CD and only 2-HP-β-CD in pure ethanol; Chl *a* in ethanol; Chl *a* in phosphate buffer solution with 10% of ethanol. For each experiment, we prepared three solutions: two identical Chl *a*/2-HP-β-CD solutions (one was irradiated and one was kept in the dark) and a solution that was only CD irradiated. For the experiments without CD, we prepared two identical Chl *a* solutions in which one was irradiated and one was not irradiated. To verify the influence that O_2 has in ROS formation, the solution was degassed under argon flow for 15 min.

Measurement. Each vial containing the solution was illuminated with a neon lamp (60 mW cm^{-2}). The solution absorption or emission spectra were recorded at different times of illumination. Uric acid absorption spectra were recorded in the range of 250–800 nm (UA λ_{max} = 290 nm in aqueous solution). SOSG emission was registered at 528 nm (λ_{ex} = 488 nm). Its maximum absorption peak was at about 500 nm. DPA fluorescence was recorded in the range of 410–450 nm (λ_{ex} = 403 nm). Its three characteristic absorption peaks were observed in the wavelength interval of 350–450 nm. 2,7-dichlorofluorescein (DCF) emission wavelength was at 525 nm (λ_{ex} = 488 nm). In the absorption spectra, the DCF peak (λ_{max} = 503 nm) can be observed. The increase in

DCF emission was followed collecting the data every 2 min. Ferricytochrome *c* presents a large absorption band in the range of 500–600 nm, in buffer and in cell medium, in which two, not very intense, peaks at 520 and 550 nm can be observed. These two peaks become more intense and welldefined when ferricytochrome *c* was reduced to ferrocytochrome *c*. Every solution, except that regarded UA and DCFH, was lighted using a cut-off glass filter (100% transmittance until 610 nm for ferricytochrome *c* and 100% transmittance until 550 nm for the other).

The UV–Vis absorption spectra were collected using the spectrophotometers Varian CARY 3 and Varian CARY 5. The fluorescent measurement, instead, was conducted using a spectrofluorimeter Varian CARY Eclipse 68.

Singlet oxygen measurements. The photogeneration of singlet oxygen ($^1O_2$) was monitored by luminescence measurements in air-saturated water solution. The samples were excited with the third harmonic of a Nd–YAG Continuum Surelite II–10 laser (355 nm, 6 ns), using quartz cells with a path length of 1.0 cm. Upon laser excitation, the emission of singlet oxygen at 1.27 μm was probed orthogonally to the exciting beam with a preamplified (low impedance) Ge-photodiode (Hamamatsu EI-P, 300 ns resolution) maintained at −196°C and coupled to a long-pass silicon filter (>1.1 μm) and an interference filter (1.27 μm). The signals from the photodiode were initially captured by a Tektronix TDS 3032 digitizer, operating in pretrigger mode and then transferred to a personal computer, controlled by Luzchem Research software operating in the National Instruments LabView 5.1 environment. The energy of the laser pulse was measured at each shot with a SPHD25 Scientech pyroelectric meter. The temporal profile of the luminescence was fitted to a single-exponential decay function with the exclusion of the initial portion of the plot, which is affected by the scattered excitation and instrumental electrical response.

Laser flash photolysis. The samples were excited with the third harmonic of a Nd–YAG Continuum Surelite II-10 laser system (pulse width 6 ns Full width at half maximum , at λ = 355 nm) and the excited solutions were analyzed at a right angle geometry using a mini mLFP-111 apparatus developed by Luzchem Research. Briefly, the monitoring beam was supplied by a ceramic xenon lamp and delivered through quartz fiber optical cables. The laser pulse was probed by fiber that synchronized the mLFP system with a Tektronix TDS 3032 digitizer operating in the pretrigger mode. The signals from a compact Hamamatsu photomultiplier were initially captured by the digitizer and then transferred to a personal computer that controlled the experiment with Luzchem software developed in the LabView 5.1 environment from National Instruments. The energy of the laser pulse was measured at each laser shot by a SPHD25 Scientech pyroelectric energy monitor. Oxygen was removed by vigorously bubbling the solutions with a constant flux of argon previously passed through a water trap. The solution (in a flow cell of 1 cm pathlength) was renewed after each laser shot. The sample temperature was 295 ± 2 K.

RESULTS

Singlet oxygen

Uric acid. The singlet oxygen has been detected using the method based on the fast reaction between UA and $^1O_2$ leading to allantoin formation. The reaction has been monitored by the decrease of the UA absorption intensity in buffer solution at 290 nm (34,35).

The UA absorbance decreasing observed in different Chl *a*/CD solutions in buffer phosphate at pH 7.5, illuminated at intervals of 15 min, is reported in Fig. 1. No decrease in UA absorption peak was observed after the illumination of the same solution in the absence of Chl *a* (data not shown).

The same study was also performed solubilizing the Chl *a* by means of ethanol, without CD, in PBS at pH 7.5 containing UA 10^{-4} M and illuminating at time interval of 10 min. In this case, the decrease in the UA absorbance intensity is steeper than that obtained in the presence of CDs (inset of Fig. 1). It suggests the possibility that CDs gave rise to a reduction in $^1O_2$ concentration

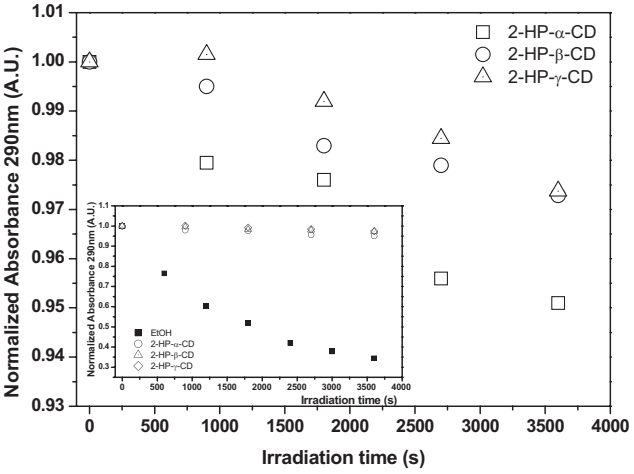

Figure 1. Time decrease of normalized absorption peak at 290 nm of UA 10^{-4} M in the presence of Chl *a* 10^{-5} M with 2-HP-α-CD 10^{-3} M (●), 2-HP-*β*-CD 10^{-3} M (○) and 2-HP-*γ*-CD 10^{-3} (Δ). Inset: comparison with Chl *a* (10^{-5} M)/AU (10^{-4} M) in ethanolic solution.

(attributable to a reduced production of $^1O_2$ and/or an increase in the quenching effects) and/or a protection of a part of the UA molecule included into CD cavity. This second hypothesis is also supported by the different behavior of UA in the presence of CDs having different size cavity: in the presence of 2-HP-α-CD, the CD having the smallest cavity size, the highest reduction in UA absorbance has been observed.

However, this method cannot be used in the presence of cell culture medium because of the overlapping of the cell culture medium and UA UV–Vis absorption spectra. Moreover in the literature, it has recently been shown that UA is not a specific probe for $^1O_2$ because it is able to react also with $O_2^{\cdot -}$ (36). Therefore, the experimental results indicate in PBS the production of $^1O_2$ and/or $O_2^{\cdot -}$ and in cell culture medium the unsuitability of this method.

Singlet oxygen sensor green. Singlet oxygen sensor green is reported in the literature as a highly selective singlet oxygen fluorescent probe probably containing a fluorescein moiety bound to an anthracene derivative. It is characterized by weak blue fluorescence peaks at 395 and 416 nm under excitation at 372 and 393 nm, respectively. SOSG has also an intense absorption band at 500 nm (28,37). The reaction with singlet oxygen gives rise to a green fluorescence under excitation at 504 nm and emission maxima at 525 nm, which has been assigned to the formation of an endoperoxide generated by the interaction of $^1O_2$ with the anthracene moiety of SOSG (38). To reduce the self-production of $^1O_2$ by SOSG, the sample illumination was performed using a 550 nm cut-off glass filter (37).

Singlet oxygen sensor green was used to detect the production of $^1O_2$ by Chl *a*/CD systems in PBS at pH 7.5, in a mixture 1:1 of PBS at pH 7.5 and deuterium oxide and, finally, in cell culture medium (Fig. 2A). Furthermore, as it is known that the inclusion or interaction of chromophore molecules with CD can alter their fluorescence, the behavior of SOSG in the presence of CD was also studied in the absence of the photosensitizer (Fig. 2B).

An initial fluorescence decrease followed by a steady fluorescence rise, as the illumination dose was further increased,

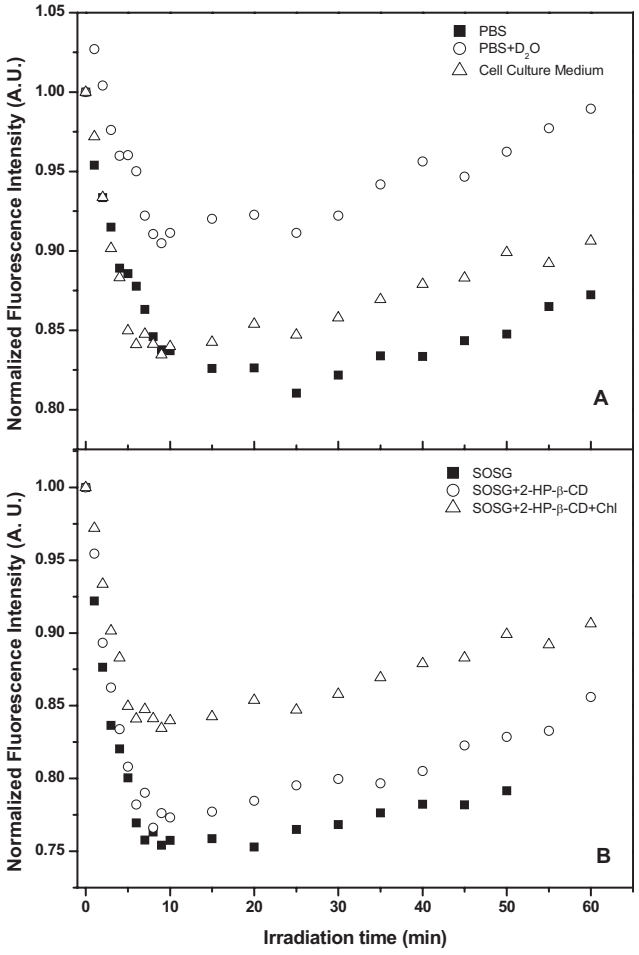

Figure 2. Time evolution of normalized fluorescence emission at 528 nm of SOSG 1.5 μM in different condition: (**A**) in the presence of Chl *a* 10^{-5} M and 2-HP-β-CD 10^{-3} M in PBS pH 7.5 (■), PBS:D_2O 1:1 (○), Cell culture medium (Δ); (**B**) in the presence of Chl *a* 10^{-5} M/2-HP-β-CD 10^{-3} M (Δ), 2-HP-β-CD 10^{-3} M (○), with no Chl *a* and 2-HP-β-CD (■).

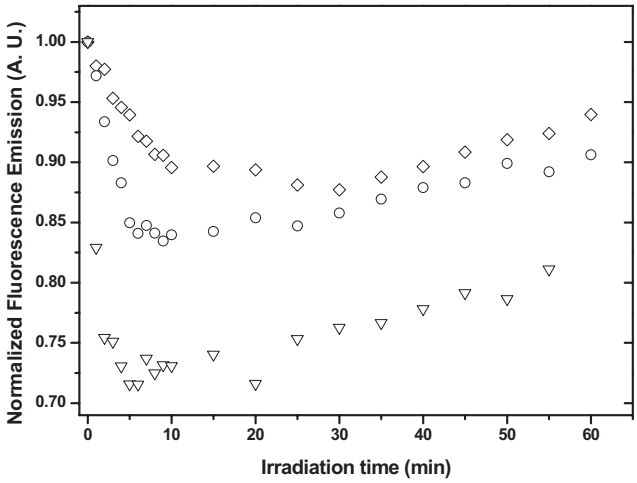

Figure 3. Time evolution of normalized fluorescence emission at 528 nm of SOSG 1.5 μM in the presence (◊),in the absence of O_2 (○) and in degassed solution (▽).

is evident in all traces of Fig. 2A,B. This initial decrease is similar to that obtained for SOSG when it is illuminated in the visible region in the absence of a PS and has already been ascribed to the occurrence of a fast intramolecular electron transfer from anthracene to fluorescein moiety, which happens after the excitation of fluorescein to its singlet excited state (37). This electron-transfer reaction, which quenches the SOSG fluorescence, competes efficiently with SOSG fluorescence until the anthracene moiety is intact. Progressively, the $^1O_2$, produced by illumination, oxidizes the anthracene moiety, making it no longer available for the deactivation pathway of the electron transfer; hence, SOSG fluorescence starts increasing. The more effective the system to produce the $^1O_2$ or to increase its life time is, the more important the competition of SOSG fluorescence will be.

Our results indicate that the presence of HP-β-CD gives rise to an increase in the self-production of $^1O_2$ by SOSG, which is much lower than the amount of singlet oxygen produced by Chl *a*/CD; therefore, the CD effect on the SOSG efficiency, as selective singlet oxygen fluorescent probe, can be neglected.

The comparison between data at the same illumination time, reported in Fig. 2A, indicates a higher $^1O_2$ production yield in cell culture medium than in phosphate buffer probably due to the presence of endogenous photosensitizers in the culture medium (39). Moreover as expected, the D_2O presence increases the $^1O_2$ life time and gives rise to the highest increase in SOSG fluorescence intensity (Fig. 2A, trace -○-).

Data reported in Fig. 2A,B were used to calculate, for each system, the $\Delta I_{max} = I_0 - I_{min}$ where I_0 is the fluorescence intensity obtained at $t = 0$, before starting the sample illumination, and I_{min} is the minimum value of fluorescence intensity, observed at the end of the first decreasing part of experimental data. The comparison between ΔI_{max} values, obtained in the different systems provides further information about the production of $^1O_2$. In the system where there is a higher production of $^1O_2$, a higher amount of anthracene moiety is oxidized and hence subtracted from the electron-transfer reaction between the anthracene–fluorescein moieties. In this case, the competition with the endoperoxide formation becomes important and the endoperoxide formation prevails over the intramolecular electron-transfer reaction. This leads to a higher I_{min} value than in the case in which higher amount of SOSG is subject to an electron-transfer reaction. In fact, the lowest and highest values of ΔI_{max}, 0.095 and 0.246, are obtained in the presence of Chl *a* 10^{-5} M and 2-HP-β-CD 10^{-3} M PBS:D_2O 1:1(○), Fig. 2A, and with no Chl *a* and 2-HP-β-CD (■) in cell culture medium, Fig. 2B, respectively.

Figure 3 shows SOSG normalized fluorescence intensity as a function of illumination time obtained in different conditions: a degassed Chl *a*/CD solution, a Chl *a*/CD solution contained in a tightly closed cuvette and in a open cuvette, where it is easy and it is not the change of air, respectively. As expected, SOSG fluorescence intensity has the highest value in the system where the O_2 concentration is the highest and where the air can be easily exchanged.

9,10-Diphenylanthracene. The $^1O_2$ production by Chl *a*/CD was also tested by means of DPA, an efficient $^1O_2$ acceptor forming endoperoxide ($DPAO_2$) with 80–100% yield through a (4 + 2) cycloaddition (40,41). $DPAO_2$ is thermostable up to about 80°C and its formation can be followed spectroscopically by observing the fluorescence intensity decrease in the range between 350 and

450 nm (λ_{exc} at 403 nm) as a function of the irradiation time (29).

The solution was illuminated at 5 min intervals using the same 550 nm cut-off glass filter used with SOSG, because also DPA is able to self-produce $^1O_2$ under irradiation (40). The measurements have been carried out both in a phosphate buffer at pH 7.5 and cell culture medium. Some preliminary studies were performed on the DPA in the absence of the PS to check if the interaction between DPA and CDs could influence our experiments. As already reported in the literature, the addition of hydroxypropyl-cyclodextrins to DPA solutions results in a small increase in DPA fluorescence intensity correlated to the formation of complex 1:1 (41). This effect is much lower than the entity of the effect produced by the PS illumination and, therefore, negligible. Both in phosphate buffer and in the cell culture medium, a decrease in DPA fluorescence intensity after the illumination of solutions containing Chl *a*/CD was observed. The dependence of this decrease on illumination time was used to perform a study of the velocity of DPA degradation promoted by its reaction with $^1O_2$ in buffer and in cell medium. In PBS, the degradation of DPA follows a first-order kinetics whose rate constant, $(8.99 \pm 0.05) \times 10^{-4}$ s^{-1}, is given by the slope of the straight line obtained graphing ln (F/F_0) as function of the illumination time, where F and F_0 are the DPA emission intensity at 500 nm at time t (illumination time) and time zero, respectively (Fig. 4).

Similar first-order kinetics were also obtained studying tryptophan degradation induced by the $^1O_2$ production by Photophrin II, its precursor hematoporphyrin, tetraphenylporphine tetrasulfonate, a synthetic porphyrin, and rose Bengal in phosphate buffer (42).

In cell culture medium, instead, DPA degradation follows a second-order kinetics. The slope of the linear trend obtained graphing 1/[DPA] as function of the illumination time (inset Fig. 4) provided the rate constant, $k = 51 \pm 1$ M^{-1} s^{-1}.

In the case of the buffer, it is possible to suppose that the first-order kinetics is the result of the following simplified kinetic scheme, already proposed for tryptophan:

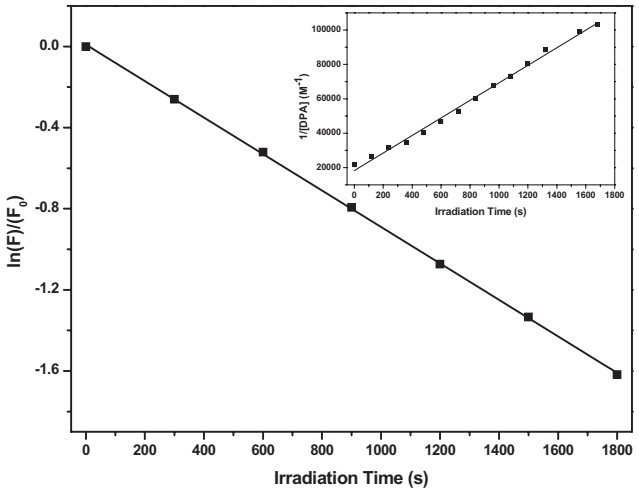

Figure 4. First-order kinetic of fluorescence quenching of DPA 25 μM registered at 500 nm in PBS in the presence of Chl *a* (10^{-5} M)/CD (10^{-3} M). Inset: Second-order kinetic of fluorescence quenching of DPA 25 μM registered at 500 nm in cell culture medium in the presence of Chl *a* (10^{-5} M)/CD (10^{-3} M).

$^1Chl + h\nu \rightarrow {}^1Chl^*$	K excitation
$^1Chl^* \rightarrow {}^3Chl^*$	k_i intersystem crossing
$^1Chl^* \rightarrow Chl + h\nu_f$	k_f fluorescence
$^3Chl^* \rightarrow Chl$	k_t triplet decay
$^3Chl^* + {}^3O_2 \rightarrow {}^3O_2 + {}^1Chl$	k_q collisional quenching
$^3Chl^* + {}^3O_2 \rightarrow {}^1O_2 + {}^1Chl$	k_Δ energy transfer
$^1O_2 \rightarrow {}^3O_2$	k_d, disactivation
$^1O_2 + DPA \rightarrow DPAO_2$	k_c, chemical quenching
$^1O_2 + DPA \rightarrow DPA + {}^3O_2$	k_p, physical quenching

which, using the stationary state approximation and assuming $(k_c + k_p)$ [DPA]<< k_d, provides the following first-order kinetic:

$$-\mathrm{d[DPA]/dt} = k'[\mathrm{DPA}]$$

$$\text{where } k' = (k_\Delta k_i k_c)/[k_d(k_{r\Delta} + k_q)(k_i + k_f)].$$

In the case of cell culture medium, the presence of many components potentially involved in various ways in the production and quenching of $^1O_2$ and hence in the DPA degradation process, probably makes the kinetic scheme much more complex. In other studies, where the intracellular generated $^1O_2$ was assessed by the quenching of DPA fluorescence, the dependence on the illumination time was not studied and the DPA fluorescence intensity was measured after extraction with chloroform/methanol (2:1) from scraped cells (43). Therefore, it is not possible, on the basis of our experimental data and studies reported in the literature, to work out a kinetic scheme able to explain the second-order kinetics experimentally obtained.

Direct detection of $^1O_2$. As all the used chemical probes for determining $^1O_2$ formation are not completely selective, even though in the literature they are often supposed to be (23,36,44,45), direct measurement of singlet oxygen 1270 nm luminescence has been conducted. In Fig. 5 are reported the singlet oxygen luminescence decay traces recorded in different systems containing Chl *a* at 10^{-5}M. From the comparison of the traces, it is clear that in general, there is a poor singlet oxygen production for all the systems in which CDs are present, in agreement with our previous results (16). This low singlet oxygen production can be attributable both to the $^1O_2$ quenching process by OH moieties of ethanol and cyclodextrins (46–48), and to the PS triplet state quenching caused by the presence of Chl *a* aggregated forms, as evidenced by the Chl *a* triplet spectra shown in the inset of Fig. 5 (49). In fact, signal of Chl *a* triplet spectrum is practically absent in the solution containing HP-β-CD (trace -○-) compared with the triplet signal in EtOH in which Chl *a* is in monomer form (trace -●-).

Singlet oxygen quenchers. In all the analyzed Chl *a*/CD systems, to confirm the singlet oxygen formation, sodium azide (NaN_3), DABCO and L-Histidine, well-known singlet oxygen quenchers have been used (50–52). The measurement (Figs. S1 and S2) has been evidenced that there is no great difference between curves obtained with and without singlet oxygen quenchers, both at 1 mM and increasing the quencher concentration to 10 mM, indicating that all quenchers do not play a protective role on the primary acceptors.

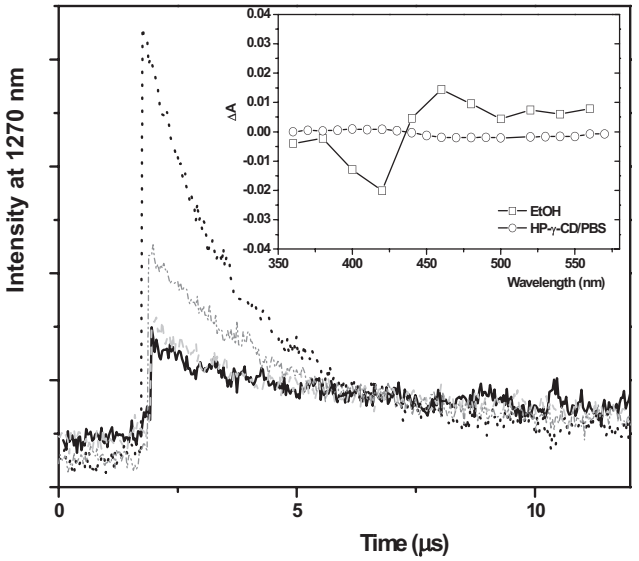

Figure 5. Singlet oxygen luminescence decay traces registered for different systems containing Chl *a* at 10^{-5} M: (—) HP-γ-CD/Buffer, (- - -) HP-γ-CD/Cell culture medium, (····) DMSO, (-···-) EtOH. Inset: Chl *a* triplet spectra recorded in EtOH (-□-) and in HP-γ-CD/Buffer (-○-).

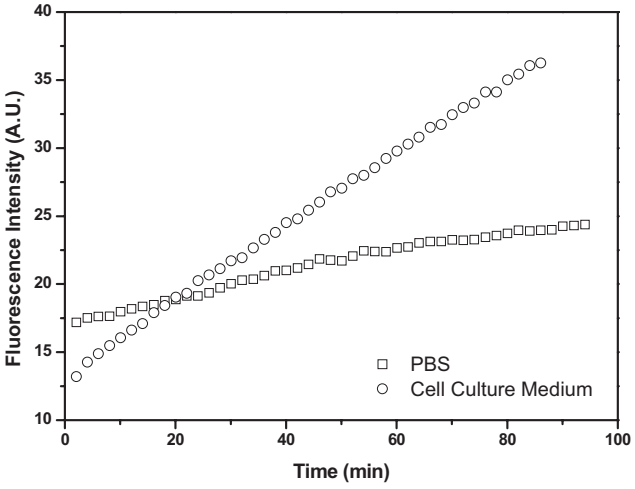

Figure 6. Time evolution of DCF fluorescence intensity registered in phosphate buffer solution and in cell culture medium for irradiated Chl *a*/2-HP-β-CD system ([Chl *a*] = 10^{-5} M and [2-HP-β-CD] = 10^{-3} M).

Table 1. Comparison light/dark of $\Delta I/\Delta t$ relative to Chl *a*/2-HP-β-CD system in different solubilization condition ([Chl *a*] = 10^{-5}M, [2-HP-β-CD] = 10^{-3}M).

	$\Delta I/\Delta t_{Light}$ (AU min^{-1})	$\Delta I/\Delta t_{Dark}$ (AU min^{-1})
Chl *a*/CD buffer	0.080 ± 0.002	0.064 ± 0.0019
Chl *a*/CD medium	0.271 ± 0.001	0.053 ± 0.001
Chl *a* ethanol	0.047 ± 0.004	0.018 ± 0.001
Chl *a*/CD ethanol	0.029 ± 0.001	0.009 ± 0.001
Chl *a* 10% ethanol	0.140 ± 0.002	0.101 ± 0.001
Chl *a*/CD (EtOH) buffer	0.051 ± 0.001	0.0463 ± 0.0004

Hydrogen peroxide

2,7-Dichlorofluorescin. DCFH is a xantenic dye that reacts with H_2O_2 in the presence of peroxidase from horseradish (HRP). DCFH, in the reduced form, is characterized by a low fluorescence intensity. It can be easily oxidized, for example by H_2O_2, forming DCF, a highly fluorescent species with an emission peak at 535 nm (λ_{ecc} = 485 nm) (31). Actually, the increase of the emission peak at 525 nm cannot always be associated with the presence of H_2O_2 in the system because of the tendency of DCFH to self-oxidize and the absence of selectively toward H_2O_2. To minimize the self-oxidation effect, DCFH is prepared in a stable nonfluorescent diacetate form (DCFH-DA), which, after activation by alkali, becomes high fluorescent when reacts with ultramicro amounts of hydrogen peroxide (53). We have prepared different type of solutions in which Chl *a*/2-HP-β-CD, Chl *a* alone and 2-HP-β-CD alone are dissolved in different media. The activated and neutralized DCFH was added to all the solutions both those irradiated for 30 min and those kept in the dark, just before beginning the fluorescence measures. This procedure was used to minimize the DCFH self-oxidation process. In this way, DCFH immediately reacts with formed H_2O_2, oxidizing to DCF. The DCF fluorescence increases at 525 nm recorded at every 2 min for 1 h are reported in Fig. 6 as example for the system Chl *a*/2-HP-β-CD in phosphate buffer solution and in cell culture medium. The slope of the linear trends registered for all examined systems are reported in Table 1.

As we can observe, $\Delta I/\Delta t$ values of the solutions in which the dye is irradiated ($\Delta I/\Delta t_{light}$) are always higher than the values obtained keeping the solution in the dark. The slight DCF emission increase registered in not illuminated solutions can be attributed to the unavoidable self-oxidation effect. The data shown in Table 1 indicate that the highest production of H_2O_2 is obtained in the solution containing Chl *a*/CD solubilized with cell culture medium.

Superoxide anion radical

Ferricytochrome c. Superoxide anion radical ($O_2^{\bullet -}$) reduces ferricytochrome *c* (Cyt Fe^{3+}) to ferrocytochrome c (Cyt Fe^{2+}), as below (30):

$$\text{Cyt Fe}^{3+} + O_2^{\bullet -} \rightarrow \text{Cyt Fe}^{2+} + O_2$$

The oxidized species presents a large absorption band between 500 and 620 nm. The formation of the reduced form gives rise to an increase in the absorbance intensity at 520 nm and at 550 nm, which have been used in this study to follow the $O_2^{\bullet -}$ formation.

Different mechanisms for the $O_2^{\bullet -}$ formation have been proposed:

$$\text{Chl} + h\nu \rightarrow {}^1\text{Chl} \rightarrow {}^3\text{Chl} \quad (1)$$

$${}^3\text{Chl} + \text{Chl} \rightarrow \text{Chl}^{\bullet -} + \text{Chl}^{\bullet +} \quad (2)$$

$$\text{Chl}^{\bullet -} + O_2 \rightarrow \text{Chl} + O_2^{\bullet -} \quad (3)$$

$$\text{Chl} + {}^1O_2 \rightarrow \text{Chl}^{+} + O_2^{\bullet -} \quad (4)$$

In alkaline solutions, the main process in facilitating $O_2^{\bullet -}$ formation is the electron transfer between the triplet state of PS and its ground state [reactions (2) and (3)]

At neutral pH and slightly acid, instead, a major role in the rate of $O_2^{\bullet -}$ formation is played by the singlet oxygen (reaction (4)) (54).

The system Chl/CD/cyt was illuminated using a neon lamp and a glass filter (which completely absorb up to 610 nm) to avoid the action of the cytochrome as a PS itself (55). The cytochrome reduction was monitored both in phosphate buffer at pH 7.5 and in cell culture medium in the presence of all CDs considered. In the cell culture medium, the Cyt Fe^{2+} formation resulted more evident (Fig. 7).

Control experiments indicated that PS and light are essential for the reduction in the cytochrome. In fact, absorption spectra of Chl *a*/2-HP-*β*-CD/Cyt in cell culture medium at different times from sample preparation, keeping the solution in darkness (Fig. 8) indicate a lower production of reduced Cyt *c* in a time much longer than that used for the experiments reported in Fig. 7.

The dependence of the increase in the absorbance intensity at 550 nm on the illumination time was used to perform a study of the kinetics of Cyt Fe^{2+} formation and consequently of $O_2^{\bullet -}$ production promoted by the PS illumination, solubilized using different CDs. In all cases, it is possible to interpret the absorbance data trends with a first-order kinetic characterized by kinetic constants having different values depending on the used CD. In particular, it is possible to group together the behavior in 2-HP-α-CD, DIMEB and TRIMEB in culture medium (Fig. 9) characterized by the lowest values of the kinetic constants: $k = (4.34 \pm 0.17) \times 10^{-5}$ s^{-1} for 2-HP-α-CD, $k = (4.43 \pm 0.38) \times 10^{-5}$ s^{-1} for DIMEB and $k = (2.48 \pm 0.15) \times 10^{-5}$ s^{-1} for TRIMEB. However, the kinetic constant values obtained in cell culture medium for 2-HP-*β*-CD and 2-HP-*γ*-CD are as follows: $k = (3.94 \pm 0.52) \times 10^{-4}$ s^{-1} for 2-HP-*γ*-CD and $k = (1.64 \pm 0.58) \times 10^{-4}$ s^{-1} for 2-HP-*β*-CD (Fig. 10).

The lowest value of the kinetic constants were obtained in the presence of the CDs having the worst Chl *a* solubilization

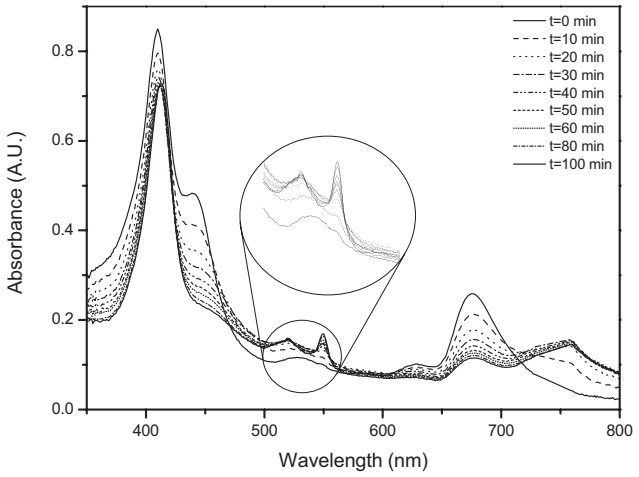

Figure 7. Time evolution of UV–Vis absorption spectra of Chl *a* 10^{-5} M/2-HP-*γ*-CD 10^{-3} M/Cyt *c* 0.1 mg mL^{-1} in cell culture medium after different illumination time.

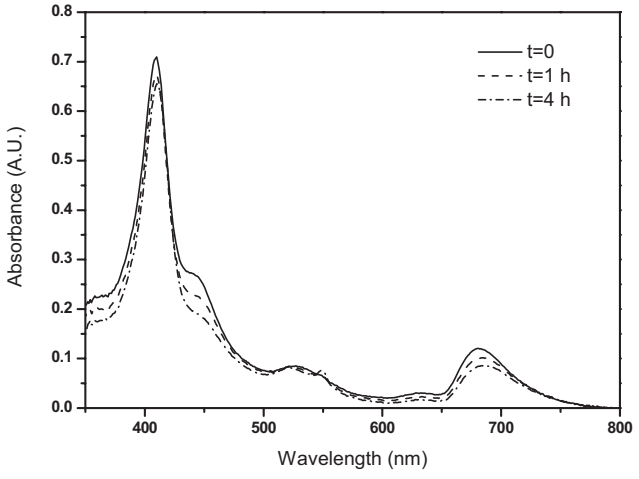

Figure 8. Time evolution of UV–Vis absorption spectra of Chl *a* 10^{-5} M/2-HP-*β*-CD 10^{-3} M/Cyt *c* 0.1 mg mL^{-1} in cell culture medium without illumination.

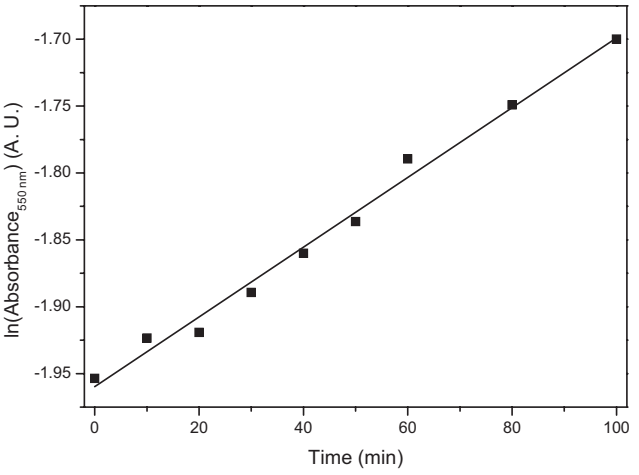

Figure 9. First-order kinetic analysis of cytochrome c reduction mediated by Chl *a* photosensitization in cell culture media. Reaction mixtures contain 10^{-5} M Chl *a* in 10^{-3} M 2-HP-α-CD with 0.1 mg mL^{-1} Cyt *c*.

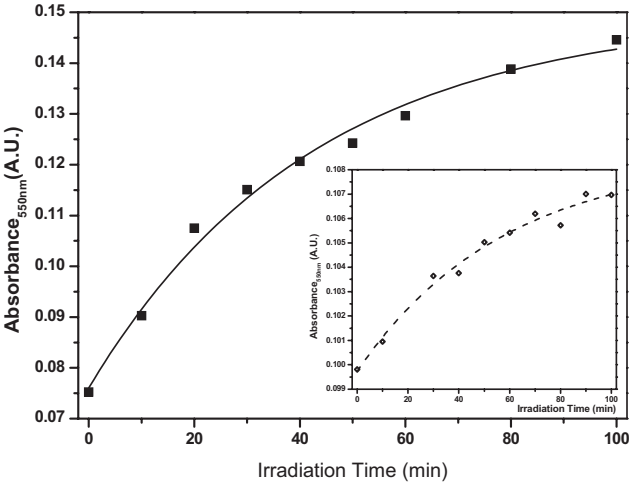

Figure 10. First-order kinetic analysis of cytochrome *c* reduction mediated by Chl *a* photosensitization in cell culture media. Reaction mixture contains 10^{-5} M Chl *a* in 10^{-3} M 2-HP-*γ*-CD with 0.1 mg mL^{-1} ferricytochrome *c*. Inset: First-order kinetic analysis of cytochrome *c* reduction mediated by Chl *a* photosensitization in PBS (Chl *a* 10^{-5} M/2-HP-*β*-CD 10^{-3} M/Cyt *c* 0.1 mg mL^{-1}).

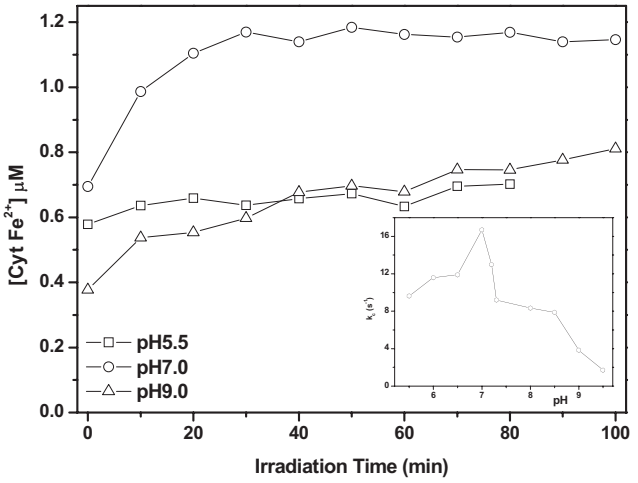

Figure 11. Cytochrome *c* reduction mediated by Chl *a* photosensitization in cell culture media as function of pH: -□- at pH 5.5, -○- at pH 7.0 and -Δ- at pH 9.0. Reaction mixture contains 10^{-5} M Chl *a* in 2-HP-*β*-CD 10^{-3} M with 0.1 mg mL^{-1} ferricytochrome *c*. Inset: first-order kinetic constants of Cyt *c* reduction mediated by Chl *a* photosensitization in cell culture media as function of pH.

power and therefore in the solutions of 2-HP-α-CD, DIMEB and TRIMEB where there is a large amount of Chl *a* aggregated (7,8). The first-order kinetic analysis of the behavior in phosphate buffer (inset of Fig. 10) has shown a higher kinetic constant, for example the k is $(2.90 \pm 0.63) \times 10^{-4}$ s^{-1} for the 2-HP-*β*-CD system. This can be attributed both to the complex matrix of cell culture medium that, containing different species, could affect the kinetic behavior of Cyt *c* reduction and also to a different pH value of the medium. To study the influence of solution pH on the rate of reduction in Cyt *c* in the presence of Chl *a*/CD inclusion complexes at a constant concentration, an investigation has been conducted varying solution pH in the range from pH 5.5 to pH 9.5. In Fig. 11, for example, the variation of Cyt *c* concentration in function of different illumination times at different solution pH is reported. At slightly acid and alkaline pH (pH 5.5, trace -□-, and pH 9.0, trace -Δ-), there are small changes in the reduced Cyt *c* concentration after illumination. In neutral solution (pH 7), instead, the reduced species is formed (trace -○- in Fig. 11). Plotting the first-order kinetic constant as a function of solution pH (inset of Fig. 11), it can be observed that the Cyt *c* reduction rate increases up to pH 7 and then decreases. This behavior can be ascribed to the presence of at least two different conformers of Cyt *c* in alkaline range of pH characterized by different reaction rates with $O_2^{\bullet-}$ (51,52). In particular, the reduced reactivity of $O_2^{\bullet-}$ toward the alkaline forms of Cyt *c* could be due to a rearrangement of Cyt *c* structure affecting the electron-transfer process (56,57). On one hand, it is possible that, at slightly acid and neutral pH, the protonation of some amino acid residues along the channel toward the Cyt *c* heme group facilitates the electron transfer speeding up the reaction of $O_2^{\bullet-}$ with protonated group (30). On the other, the conformational change of Cyt *c* at alkaline pH is accompanied by a decreasing of the reduction potential with increasing pH, resulting in a reduced reactivity (58,59).

After the pH effect, also the change in the Chl *a* concentration was studied. Reducing the concentration of PS at 5×10^{-6} M, the amount of Cyt Fe^{2+} formed resulted lower than that obtained at Chl *a* 10^{-5} M. However, no significant differences were observed at Chl *a* concentrations between 7.5×10^{-6} and $< 10^{-5}$ M (Data not shown).

The high tendency of Chl *a* to aggregate at increasing of its concentration also in the presence of high CD concentration makes difficult to extend this study to a wider range of concentration.

At last, to obtain a conclusive proof of the involvement of $O_2^{\bullet-}$ in the Cyt Fe^{3+} reduction, the system Chl/CD/cyt has been illuminated in the presence of active superoxide dismutase from horseradish (SOD). As no changes have been obtained in the Cyt *c* absorption spectra at 520 and 550 nm (data not shown), in the presence of SOD, it is possible to conclude that the formation of Cyt Fe^{2+} is actually due to the involvement of $O_2^{\bullet-}$ (60).

CONCLUSION

The photodynamic activity of the system Chl *a*/CD has been studied successfully in PBS and in cell culture medium using mainly the chemical detection of ROS. Experimental results indicate overall that $^1O_2$, H_2O_2 and $O_2^{\bullet-}$ are the main ROS produced by the studied system. In particular, the $^1O_2$ production in PBS and in cell culture medium has been tested using UA, SOSG, DPA as primary acceptors and direct detection of $^1O_2$ NIR-luminescence decay. The overlapping of the cell culture medium and UA UV–Vis absorption spectra makes the use of UA as primary acceptor in cell culture medium impossible, but not in PBS. SOSG and DPA methods both indicate a higher $^1O_2$ production in cell culture medium than in phosphate buffer probably due to the presence of endogenous photosensitizers in the cell medium. The kinetic analysis of DPA degradation promoted by its reaction with $^1O_2$ evidences first-order kinetics in PBS and second-order kinetics in cell culture medium. Also, the direct measurement by means of the $^1O_2$ 1270 nm luminescence decay has evidenced the production of singlet oxygen even if in a small amount.

The method for the detection of $O_2^{\bullet-}$ based on its redox reaction with Cyt *c* Fe^{3+} reveals the superoxide radical anion production in all Chl *a*/CD systems with a first-order kinetics. The lowest value of the kinetic constants has been obtained in the presence of the CDs having the worst Chl *a* solubilization power and therefore in the solutions of 2-HP-α-CD, DIMEB and TRIMEB where there is a large amount of Chl *a* aggregated.

Evidence of the H_2O_2 formation by Chl *a*/CD illumination has been obtained using the DCFH method both in cell culture medium and PBS.

The overall results obtained in this article and in a previous one (11) induce us to hypothesize that Type-I pathways could prevail to Type-II pathway in the ROS production.

In fact in a previous study of ours, in which the photoactivity of these systems were tested on Jurkat cells, notwithstanding a weak production of singlet oxygen, Chl *a*/CD complexes are able to kill malignant cells only when they are illuminated (11). It results that there is a remarkable ROS production, enough to promote cell death and that these ROS are mainly radicals, produced by Type-I pathways and not by Type II, which is the pathway involved in the singlet oxygen production.

Analogous indications have been obtained in this article by means of the use of different ROS quenchers (NaN_3, DABCO, L-histidine, SOD) in agreement with procedures suggested in

the literature (riferimenti vari). In general, in the case of $^1O_2$ quenchers (61,62), a significative decrease in the lifetime of singlet oxygen with different quenching rate constants is observed. Whereas, superoxide dismutase is known to catalyze the following dismutation reaction

$$O_2^{\bullet -} + O_2^{\bullet -} + 2H^- \longrightarrow H_2O_2 + O_2$$

with quenching of superoxide anion species and H_2O_2 production.

Our experimental results indicate that the presence of singlet oxygen quenchers does not affect the behavior of used ROS chemical probes (Data in Supporting Information). This suggests that $^1O_2$ is produced in small amount and it is not the major source of radical ROS implying thus that Type-I mechanism is dominant. A confirmation of this hypothesis is provided also by the very low Chl *a* triplet signal recorded in solution containing CDs (inset of Fig. 5). Also, the use of SOD provides indication of a prevalence of a photodynamic mechanism of Type I. In fact, no changes have been obtained in the Cyt *c* absorption spectra in the presence of SOD, indicating that the formation of Cyt Fe^{2+} is due to the involvement of $O_2^{\bullet -}$, produced by a Type-I pathway (60).

Then, we may conclude that the photodynamic activity of Chl *a*/CD systems occurred mainly *via* the Type-I mechanism.

Acknowledgements—This study was supported by COFIN-MIUR2008 grants "Architetture ibride multifunzionali basate su biomolecole per applicazioni nel campo della sensoristica, della conversione di energia e del biomedicale." We gratefully acknowledge the skillful and excellent technical assistance of Sergio Nuzzo.

SUPPORTING INFORMATION

Additional Supporting Information may be found in the online version of this article:

Figure S1. Time evolution of normalized fluorescence emission recorded at 528 nm of SOSG 1.5 M in PBS solution (pH 7.5) containing Chl *a* 10^{-5} M and 2-HP-β-CD 10^{-3} M with different quenchers at concentration of 10 mM.

Figure S2. Time evolution of normalized fluorescence emission recorded at 500 nm of DPA 25 μM in PBS solution (pH 7.5) containing Chl *a* 10^{-5} M and 2-HP-β-CD 10^{-3} M with different quenchers at concentration of 10 mM.

Chart S1. Chemical structures of primary acceptors and singlet oxygen quenchers used in this article.

Please note: Wiley-Blackwell are not responsible for the content or functionality of any supporting materials supplied by the authors. Any queries (other than missing material) should be directed to the corresponding author for the article.

REFERENCES

1. Jori, G. (2006) Photodynamic therapy of microbial infections: State of the art and perspectives. *J. Environ. Pathol. Toxicol. Oncol.* **25**, 505–520.
2. Séguier, S., S. L. S. Souza, A. C. V. Sverzut, A. R. Simioni, F. L. Primo, A. Bodineau, V. M. A. Corrêa, B. Coulomb and A. C. Tedesco (2010) Impact of photodynamic therapy on inflammatory cells during human chronic periodontitis. *J. Photochem. Photobiol. B: Biol.* **101**, 348–354.
3. Bredell, M. G., E. Besic, C. Maake and H. Walt (2010) The application and challenges of clinical PD–PDT in the head and neck region: A short review. *J. Photochem. Photobiol. B: Biol.* **101**, 185–190.
4. Henderson, B. W. and T. J. Dougherty (1992) How does photodynamic therapy work? *Photochem. Photobiol.* **55**, 155–157.
5. Foote, C. S. (1991) Definition of type I and Type II photosensitized oxidation. *Photochem. Photobiol.* **54**, 659.
6. DeRosa, M. C. and R. J. Crutchley (2002) Photosensitized singlet oxygen and its applications. *Coord. Chem. Rev.* **233/234**, 351–371.
7. Ebermann, R., G. Alth, M. Kreitner and A. Kubin (1996) Natural products derived from plants as potential drugs for the photodynamic destruction of tumor cells. *J. Photochem. Photobiol. B: Biol.* **36**, 95–97.
8. Agostiano, A., L. Catucci, P. Cosma and P. Fini (2003) Aggregation processes and photophysical properties of chlorophyll a in aqueous solutions modulated by the presence of cyclodextrins. *Phys. Chem. Chem. Phys.* **5**, 2122–2128.
9. Agostiano, A., L. Catucci, M. Castagnolo, D. Colangelo, P. Cosma, P. Fini and M. Della Monica (2002) Interaction between chlorophyll a and β-cyclodextrin derivatives in aqueous solutions. Spectroscopic and calorimetric study. *J. Therm. Anal. Calorimetry* **70**, 115–122.
10. Cosma, P., L. Catucci, P. Fini, P. L. Dentuto, A. Agostiano, N. Angelini and L. Monsù Scolaro (2006) Tetrakis (4-pyridy1)porphyrin supramolecular complexes with cyclodextrins in aqueous solution. *Photochem. Photobiol.* **82**, 563–569.
11. Dentuto, P. L., L. Catucci, P. Cosma, P. Fini, A. Agostiano, S. Hackbarth, F. Rancan and B. Roeder (2007) Cyclodextrin/chlorophyll a complexes as supramolecular photosentizers. *Bioelectrochemistry* **70**, 39–43.
12. Kuronen, P., K. Hyvgrinen, P. H. Hynninen and I. Kipelãinen (1993) High-performance liquid chromatographic separation and isolation of the methanolic allomerization products of chlorophyll a. *J. Chromatogr. A* **654**, 93–104.
13. Hynninen, P. H. (1991) Chemistry of chlorophyll: Modification. In *Chlorophylls* (Edited by H. Scheer), pp. 145–209. CRC Press, Boca Raton, FL.
14. Watanabe, T., H. Mazaki and M. Nakazato (1987) Chlorophyll a/a′ epimerization in organic solvents. *Biochim. Biophys. Acta* **892**, 197–206.
15. Shen, S.-C., H. Yunhsu, C. Nenghuang and J. Swi-Beawu (2010) Color loss in ethanolic solutions of chlorophyll a. *J. Agric. Food Chem.* **58**, 8056–8060.
16. Dentuto, P. L., L. Catucci, P. Cosma, P. Fini, A. Agostiano, L. D'Accolti, C. C. Trevithick-Sutton and C. S. Foote (2005) Effect of cyclodextrins on the physicochemical properties of chlorophyll a in aqueous solution. *J. Phys. Chem. B.* **109**, 1313–1317.
17. Cosma, P., P. Fini, S. Rochira, L. Catucci, M. Castagnolo, A. Agostiano, R. Gristina and M. Nardulli (2008) Phototoxicity and cytotoxicity of chlorophyll a/cyclodextrins complexes on Jurkat cells. *Bioelectrochemistry* **74**, 58–61.
18. Ochsner, M. (1997) Photophysical and photo biological processes in the photodynamic therapy of tumours. *J. Photochem. Photobiol. B: Biol.* **39**, 1–18.
19. Leroy-Lechat, F., D. Wouessidjewe, J.-P. Andreux, F. Puisieux and D. Duchêne (1994) Evaluation of the cytotoxicity of cyclodextrins and hydroxypropylated derivatives. *Int. J. Pharm.* **101**, 97–103.
20. Kiss, T., F. Fenyvesi, I. Bácskay, J. Váradi, É. Fenyvesi, R. Iványi, L. Szente, Á. Tósaki and M. Vecsernyés (2010) Evaluation of the cytotoxicity of β-cyclodextrin derivatives: Evidence for the role of cholesterol extraction. *Eur. J. Pharm. Sci.* **40**, 376–380.
21. Snyrychova, I. (2010) Improvement of the sensitivity of EPR spin trapping in biological systems by cyclodextrins, A model study with thylakoids and photosystem II particles. *Free Radical Biol. Med.* **48**, 264–274.
22. Shi, H., G. Timmins, M. Monske, A. Burdick, B. Kalyanaraman, Y. Liu, J.-L. Clément, S. Burchiel and K. J. Liu (2005) Evaluation of spin trapping agents and trapping conditions for detection of cell-generated reactive oxygen species. *Arch. Biochem. Biophys.* **437**, 59–68.
23. Baier, J., T. Maisch, M. Maier, M. Landthaler and W. Bäumler (2007) Direct detection of singlet oxygen generated by UVA irradiation in human cells and skin. *J. Invest. Dermatol.* **127**, 1498–1506.

24. Niedre, M., M. S. Patterson and B. C. Wilson (2002) Direct near-infrared luminescence detection of singlet oxygen generated by photodynamic therapy in cells in vitro and tissues in vivo. *Photochem. Photobiol.* **754**, 382–391.
25. Ames, B. N., R. Cathcart, E. Schwiers and P. Hochsteint (1981) Uric acid provides an antioxidant defense in humans against oxidant- and radical-caused aging and cancer, A hypothesis. *Proc. Natl Acad. Sci. USA* **78**, 6858–6862.
26. Dunlap, W. C., Y. Yamamoto, M. Inoue, M. Kashiba-Iwatsuki, M. Yamaguchi and K. Tomita (1998) Uric acid photo-oxidation assay, in vitro comparison of sunscreening agents. *Int. J. Cosmetic Sci.* **20**, 1–18.
27. Cavalcante, R. S., H. Imasato, V. S. Bagnato and J. R. Perussi (2009) A combination of techniques to evaluate photodynamic efficiency of photosensitizers. *Laser Phys. Lett.* **6**, 64–70.
28. Flors, C., M. J. Fryer, J. Waring, B. Reeder, U. Betchold, P. M. Mullineaux, S. Nonell, M. T. Wilson and N. R. Baker (2006) Imaging the production of singlet oxygen in vivo using a new fluorescent sensor, singlet oxygen sensor green. *J. Exp. Bot.* **57**, 1725–1734.
29. Lavi, A., H. Weiman, R. T. Holmes, K. M. Smith and B. Ehrenberg (2002) The depth of porphyrin in a membrane and the membrane's physical properties affect the photosensitizing efficiency. *Biophys. J .* **82**, 2101–2110.
30. Butler, J., G. G. Jayson and A. J. Swallow (1975) The reaction between the superoxide anion radical and cytochrome c. *Biochim. Biophys. Acta* **408**, 215–222.
31. Rota, C., C. F. Chignell and R. P. Mason (1999) Evidence for free radical formation during the oxidation of 2′-7′-dichlorofluorescin to the fluorescent dye 2′-7′-dichlorofluorescein by horseradish peroxidase, possible implications for oxidative stress measurements. *Free Radical Biol. Med.* **27**, 873–881.
32. Omata, T. and N. A. Murata (1980) Rapid and efficient method to prepare chlorophyll a and b from leaves. *Photochem. Photobiol.* **31**, 183–185.
33. Olivier, D., S. Douillard, I. Lhommeau, E. Bigot and T. Patrice (2009) Secondary oxidants in human serum exposed to singlet oxygen: The influence of hemolysis. *Photochem. Photobiol. Sci.* **8**, 1476–1486.
34. Ammann, E. C. B. and V. H. Lynch (1966) Purine metabolism by unicellular algae III. The photochemical degradation of uric acid by chlorophyll. *Biochim. Biophys. Acta* **120**, 181–182.
35. Spikes, J. D. (1975) Porphyrins and related compounds as photodynamic sensitizers. *Ann. N. Y. Acad. Sci.* **244**, 496–508.
36. Montaña, M. P., W. A. Massad, F. Amat-Guerri and N. A. García (2008) Scavenging of riboflavin-photogenerated oxidative species by uric acid, xanthine or hypoxanthine, A kinetic study. *J. Photochem. Photobiol. A: Chem.* **193**, 103–109.
37. Ragas, X., A. Jimenez-Banzo, D. Sanchez-Garcia, X. Batllori and S. Nonell (2009) Singlet oxygen photosensitisation by the fluorescent probe singlet oxygen sensor green. *Chem. Commun.* 2920–2922.
38. Tanaka, K., T. Miura, N. Umezawa, Y. Urano, K. Kikuchi, T. Higuchi and T. Nagano (2001) Rational design of fluorescein-based fluorescence probes. Mechanism-based design of a maximum fluorescence probe for singlet oxygen. *J. Am. Chem. Soc.* **123**, 2530–2536.
39. Davies, M. J. (2003) Singlet oxygen-mediated damage to proteins and its consequences. *Biochem. Biophys. Res. Commun.* **305**, 761–770.
40. Lee, H.-Y., S. Chen, M.-H. Zhang and T. Shen (2003) Studies on the synthesis of two hydrophilic hypocrellin derivatives with enhanced absorption in the red spectral region and on their photogeneration of $O_2^{\cdot\,-}$ and $O_2{}^1\Delta_g$. *J. Photochem. Photobiol. B: Biol.* **71**, 43–50.
41. Slaventinska, L., J. Mosinger and P. Kubat (2008) Supramolecular carriers of singlet oxygen, photosensitized formation and thermal decomposition of endoperoxides in the presence of cyclodextrins. *J. Photochem. Photobiol. A: Chem.* **195**, 1–9.
42. Gottfried, V., D. Peled, J. W. Winkelman and S. Kimel (1988) Photosensitizers in organized media, singlet oxygen production and spectral properties. *Photochem. Photobiol.* **48**, 157–163.
43. Klotz, L.-O., C. Pellieux, K. Briviba, C. Pierlot, J.-M. Aubry and H. Sies (1999) Mitogen-activated protein kinase p38-, JNK-, ERK-) activation pattern induced by extracellular and intracellular singlet oxygen and UVA. *Eur. J. Biochem.* **260**, 917–922.
44. Soh, N. (2006) Recent advances in fluorescent probes for the detection of reactive oxygen species. *Anal. Bioanal. Chem.* **386**, 532–543.
45. Fischer, F., G. Graschew, H.-J. Sinn, W. Maier-Borst, W. J. Lorenz and P. M. Schlag (1998) A chemical dosimeter for the determination of the photodynamic activity of photosensitizers. *Clin. Chim. Acta* **274**, 89–104.
46. Mosinger, J., M. Deumié, K. Lang, P. Kubát and D. M. Wagnerová (2000) Supramolecular sensitizer: Complexation of meso-tetrakis (4-sulfonatophenyl) porphyrin with 2-hydroxypropyl-cyclodextrins. *J. Photochem. Photobiol. A: Chem.* **130**, 13–20.
47. Bourdelande, J. L., J. Fonta, G. Marques, A. A. Abdel-Shafi, F. Wilkinson and D. R. Worrall (2001) On the efficiency of the photosensitized production of singlet oxygen in water suspensions of a trisbipyridy(l) ruthenium(II) complex covalently bound to an insoluble hydrophilic polymer. *J. Photochem. Photobiol. A: Chem.* **138**, 65–68.
48. Clennan, E. L., L. J. Noe, E. Szneler and T. Wen (1990) Hydrazine: New charge-transfer physical quenchers of singlet oxygen. *J. Am. Chem. Soc.* **112**, 5080–5085.
49. Alfano, A. J., M. S. Showell and F. K. Fong (1985) Triplet-state decay kinetics of hydrated chlorophyll complexes. *J. Chem. Phys.* **82**, 765–772.
50. Hasty, N., P. B. Merkel, P. Radlick and D. R. Kearns (1972) Role of azide in singlet oxygen reactions: Reaction of azide with singlet oxygen. *Tetrahedron Lett.* **1**, 49–52.
51. Yamakoshi, Y., N. Umezawa, A. Ryu, K. Arakane, N. Miyata, Y. Goda, T. Masumizu and T. Nagano (2003) Active oxygen species generated from photoexcited fullerene (C60) as potential medicines: $O_2^{-\bullet}$ versus $^1O_2$. *J. Am. Chem. Soc.* **125**, 12803–12809.
52. Gorman, A. A. and M. A. J. Rodgers (1992) Current perspectives of singlet oxygen detection in biological environments. *J. Photochem. Photobiol. B: Biol.* **14**, 159–176.
53. Keston, A. S. and R. Brandt (1965) The fluorimetric analysis of ultramicro quantities of hydrogen peroxide. *Anal. Biochem.* **11**, 1–5.
54. Hadjur, C. and P. Jardon (1995) Quantitative analysis of superoxide anion radicals photosensitized by hypericin in a model membrane using the cytochrome c reduction method. *J. Photochem. Photobiol. B: Biol.* **29**, 147–156.
55. Bazin, M., F. Bosca, M. L. Marin, M. A. Miranda, L. K. Patterson and R. Santus (2000) A laser flash photolysis and pulse radiolysis study of primary photochemical processes of flumequine. *Photochem. Photobiol.* **72**, 451–457.
56. Yash, P. M. (1968) Conformation of cytochromes. III. Effect of urea, temperature, extrinsic ligands, and pH variation on the conformation of horse heart ferricytochrome c. *Biochemistry* **7**, 765–776.
57. Greenwood, C. and G. Palmer (1965) Evidence for the existence of two functionally distinct forms of cytochrome c monomer at alkaline pH. *J. Biol. Chem.* **240**, 3660–3663.
58. Simic, M. G., I. A. Taub, J. Tocci and P. A. Hurwitz (1975) Free radical reduction of ferricytochrome-c. *Biochem. Biophys. Res. Commun.* **62**, 161–167.
59. Koppenol, W. H., K. J. H. Van Buuren, J. Butler and R. Braams (1976) The kinetics of the reduction of cytochrome c by the superoxide anion radical, *Biochim. Biophys. Acta* **449**, 157–168.
60. Bazin, M., L. K. Patterson, J. C. Ronfard-Haret and R. Santus (1988) Superoxide dismutase as an amplifier of the chemical reactivity of porphyrin radical-cations. *Photochem. Photobiol.* **48**, 177–180.
61. Tavares, A., S. R. S. Dias, C. M. B. Carvalho, M. A. F. Faustino, J. P. C. Tomè, M. G. P. M. Neves, A. C. Tomè, J. A. S. Cavaleiro, A. Cunha, N. C. M. Gomes, E. Alves and A. Alemida (2011) Mechanisms of photodynamic inactivation of a Gram-negative recombinant bioluminescent bacterium by cationic porphyrins. *Photochem. Photobiol. Sci.* **10**, 1659–1669.
62. Li, M. Y., C. S. Cline, E. B. Koker, H. H. Carmichael, C. F. Chignell and P. Bilski (2001) Quenching of singlet molecular oxygen ($^1O_2$) by azide anion in solvent misture. *Photochem. Photobiol.* **74**, 760–764.